Heliyon 10 (2024) e24861

Contents lists available at ScienceDirect

Heliyon

journal homepage: www.cell.com/heliyon

Research article

Immune landscape of hepatocellular carcinoma tumor microenvironment identifies a prognostic relevant model

Hongru Cao [d,1], Ping Huang [e,1], Jiawei Qiu [c], Xiaohui Gong [b,c,*], Hongfei Cao [a,**]

[a] Department of Gastroenterology, Affiliated Hospital of Chifeng University, Chifeng City, Inner Mongolia, 024000, PR China
[b] Department of Emergency Medicine, Affiliated Hospital of Chifeng University, Chifeng City, Inner Mongolia, 024000, PR China
[c] Institute of Cardiovascular Disease of Chifeng University, Chifeng City, Inner Mongolia, 024000, PR China
[d] Department of Nephrology, Affiliated Hospital of Chifeng University, Chifeng City, Inner Mongolia, 024000, PR China
[e] Infectious Disease Prevention and Control Hospital of Chifeng City, Chifeng City, Inner Mongolia, 024000, PR China

ARTICLE INFO

Keywords:
Hepatocellular carcinoma (HCC)
Tumor microenvironment (TME)
Immune cell infiltration
Prognostic immune risk score (pIRG)
LASSO cox regression

ABSTRACT

Background: Various studies highlighted that immune cell-mediated inflammatory processes play crucial roles in the progression and treatment of hepatocellular carcinoma (HCC). However, the immune microenvironment of HCC is still poorly characterized. Exploring the role of immune-related genes (IRGs) and describing the immune landscape in HCC would provide insights into tumor-immune co-evolution along HCC progression.

Methods: We integrated the datasets with complete prognostic information from the Cancer Genome Atlas (TCGA) database and GEO DataSets (GSE14520, GSE76427, and GSE54236) to construct a novel immune landscape based on the Cibersort algorithm and reveal the prognostic signature in HCC patients.

Results: To describe the tumor microenvironment (TME) in HCC, immune infiltration patterns were defined using the CIBERSORT method, and a prognostic signature contains 5 types of immune cells, including 3 high-risk immune cells (T.cells. CD4. memory. resting, Macrophages.M0, Macrophages.M2) and 2 low-risk immune cells (Plasma. cells, T.cells.CD8), were finally constructed. A novel prognostic index, based on prognostic immune risk score (pIRG), was developed using the univariate Cox regression analyses and LASSO Cox regression algorithm. Furthermore, the ROC curve and KM curve showed that the TME signatures had a stable value in predicting the prognosis of HCC patients in the internal training cohort, internal validation, and external validation cohort. Differential genes analysis and qPCR experiment showed that the expression levels of AKR1B10, LAPTM4B, MMP9, and SPP1 were significantly increased in high-risk patients, while the expression of CD5L was lower. Further analysis found that AKR1B10 and MMP9 were associated with higher M0 macrophage infiltration, while CD5L was associated with higher plasma cell infiltration.

Conclusions: Taken together, we performed a comprehensive evaluation of the immune landscape of HCC and constructed a novel and robust prognostic prediction model. AKR1B10, LAPTM4B,

* Corresponding author. Department of Emergency Medicine, Affiliated Hospital of Chifeng University, Chifeng City, Inner Mongolia, 024000, PR China.
** Corresponding author. Affiliated Hospital of Chifeng University, Wangfu Street No.42, Songshan District, Chifeng City, Inner Mongolia, 024000, PR China.
E-mail addresses: gxh708@163.com (X. Gong), cfsyychf@163.com (H. Cao).
[1] These authors have contributed equally to this work and share first authorship.

https://doi.org/10.1016/j.heliyon.2024.e24861
Received 4 August 2023; Received in revised form 10 January 2024; Accepted 16 January 2024
Available online 24 January 2024

MMP9, SPP1, and CD5L were involved in important processes in the HCC tumor microenvironment and were expected to become HCC prediction markers and potential targets of treatment.

1. Introduction

Hepatocellular carcinoma (HCC), accounting for approximately 90 % of the incidence of all liver cancers, represents the third leading cause of cancer-related deaths worldwide [1,2]. Moreover, its morbidity and mortality are steadily increasing, and its global burden is predicted to increase by more than 55 % by the year 2040 [3,4]. Despite a degree of progress in diagnostics and therapy, HCC diagnosed at an advanced stage or with progression after locoregional therapy has a poor prognosis, and the 5-year survival rate of HCC remains very low [5–9]. Only one drug (sorafenib, a multikinase inhibitor) is approved for the treatment of advanced HCC, and these patients treated with sorafenib achieve minimal therapeutic benefit with an improvement in overall survival of only 3 months [10,11]. Although sorafenib is considered the only first-line systemic chemotherapeutic drug that can significantly improve the overall survival (OS) rate of patients with advanced HCC, it only led to a limited survival benefit [12–15]. Therefore, it is imperative to explore novel therapeutic targets and prognostic models for the prevention and treatment of HCC.

Various studies reported that immunotherapies have clinical benefits for many cancer indications. However, immunotherapies in HCC benefit only up to 20 % of the patients who respond to immune checkpoint inhibitors [14–17]. As an inflammation-related tumor, the tumor microenvironment (TME) is strongly associated with treatment efficacy in HCC. The TME is a complex dynamic system with diverse populations of immune cell subsets, extracellular matrix, and various cytokines, which play critical roles in tumor initiation, progression, and responses to immunotherapy treatment [16,18–20]. The specific TME of HCC can influence immune tolerance and evasion by mixed mechanisms. Many ongoing clinical trials promote the development of tumor immunotherapies against HCC [12,21,22]. For instance, biomarkers studies from HCC patients demonstrated that Tumor-associated macrophages (TAMs) prevent T cells from recognizing and killing cancer cells, while cytolytic activity of $CD8^+$ T cells predicts immunotherapies response [18,23–26]. These studies indicate the crucial role of immunology in HCC management, although the molecular mechanisms and sensitive biomarkers remain to be further explored.

Although studies have established immune-based signatures to predict HCC patients' outcomes, the fundamental understanding of the subtle cellular and molecular landscapes in HCC remains elusive [27,28]. These predictive accuracies of most signatures are still insufficient for clinical practice, and there is an urgent need for more reliable and accurate signatures to predict the survival as well as the immunotherapy response of HCC patients. Recently, studies have emerged to characterize immune cell subsets in the TME, including mass cytometry studies and Single Cell RNA sequencing studies on colorectal cancer, and kidney cancer et al., paving the way for such studies in HCC. Benefiting from the emergence and development of public large-scale gene expression datasets, many molecular mechanisms related to patient survival have been identified [25,29–32]. Therefore, combined analysis of these various databases may represent a preferred approach toward achieving an in-depth understanding of the immune landscape of HCC. Here we systematically revealed the cell composition, functional states, and cellular interactions of immune cells in HCC tumors. Concurrently, we also uncovered TME-related transcriptome-immune networks and the distinct molecular pathways involved in dictating HCC progression and immune status, which can be harnessed as a predictive signature for HCC progression and prognosis.

2. Materials and methods

2.1. Data source

After searching the data set for the cohort with complete clinicopathological parameters, TCGA, GSE14520, GSE76427, and GSE54236 were included in this study. Transcriptome profile and survival data of HCC samples were downloaded from TCGA (http://cancergenome.nih.gov/) and GEO (http://www.ncbi.nlm.nih.gov/geo/). The corresponding clinical data and survival outcomes were also collected, and those patients with an overall survival time of <30 days were excluded due to other possible causes of mortality [28]. For the mRNA expression datasets in TCGA, the Fragments per Kilobase Million (FPKM) value was used to generate the Transcripts per Kilobase Million (TPM) and further subjected to log2 transformation for normalization. Clean reads were obtained from the original data after quality control using fastq (v0.20.0) and then filtered by mRNA from SILVA (v138.1) using bowite2 (v2.2.4). The remaining data were finally aligned to the human genome (GRCh38.101) using hisat2 (v2.2.1). Gene quantification was performed using featureCounts (v2.0.1).

After background correction, normalization, and removal of duplicate probes, the obtained datasets were uploaded to the Cibersort website (https://cibersort.stanford.edu/), after 1000 repeated calculations, patients with $p < 0.05$ were selected for further study. Finally, a total of 131 patients in TCGA and 167 patients in three datasets in GEO were used for further analysis. Perl and R in R software are used to evaluate the samples.

2.2. CIBERSORT

CIBERSORT is a machine-learning approach for characterizing the cell composition of a tumor biopsy from gene expression data (http://cibersort.stanford.edu) and is a useful method for the high-throughput characterization of various cell types, such as tumor-infiltrating leukocytes. The patient's OS status and time were obtained from GEO and TCGA cohorts. Here, we used the

CIBERSORT method to calculate the proportions of 16 types of immune cells related to the patient's life cycle.

2.3. Univariate cox regression analysis

To determine the prognostic value of 16 types of immune cells that were obtained from Cibersort, we performed a univariate analysis. Univariate COX regression initially screened immune cells related to the patient's OS ($p < 0.05$).

2.4. Establishment of the lasso-cox signature

Compared with the traditional Cox regression model, LASSO-based Cox regression decreases the variables of the model, avoids overfitting and collinearity and has clinical significance. Here, LASSO-Cox regression analysis, including 16 type immune cells, was performed to identify immune cells' HCC prognosis associated with HCC prognosis. Firstly, 131 TCGA patients enrolled in the study were randomly assigned to a 1:1 training set and a verification set. The immune cells with significance in univariate analysis were included in the minimum absolute contraction penalty Cox regression model and the selection operator Lasso Cox regression model. To obtain the most accurate models for the tested data sample, ten times cross-validation was carried out, and the most significant genes were selected to construct the prognosis model.

$$\min_{\omega} \sum_{j=1}^{m} \left(y_j - \sum_{i=1}^{n} \chi_{ji} \omega_i \right)^2, \text{s.t.} \sum_{i=1}^{n} |\omega_i| \leq \lambda$$

2.5. ROC curve

We used the R software package "pROC" to generate the receiver operating characteristic curve (ROC) and calculate the area under the curve (AUC). The "Survival ROC" package was applied to perform survival analysis and draw the survival curves.

2.6. KEGG analysis

To gain more mechanistic insights into the underlying biology of the condition being studied, analyzing high-throughput molecular measurements at the functional level has become more and more appealing. Especially, the knowledge base-driven pathway analysis is becoming the first choice for many investigators, which mainly exploit pathway knowledge in public repositories, such as the Kyoto Encyclopedia of Genes and Genomes (KEGG). Here, we used the Kyoto Encyclopedia of Genes and genomes (KEGG) analysis of the package clusterProfiler in R to determine the biological pathways of different groups of genes associated with the model.

2.7. qRT-PCR

TRIzol® reagent (Invitrogen; Thermo Fisher Scientific, Inc.) was used to extract Total RNA from HCC cell lines and normal liver cell lines. The RNA was reversely transcribed into cDNA with the cDNA Kit (Thermo Fisher Scientific). Primer sequences are listed in Table 1.

2.8. Statistical analysis

Continuous variables were analyzed by student t-test or nonparametric test. The chi-square test or Fisher's accurate test was used to analyze the classified variables. The R software package was used for survival analysis. R packet replication was used in univariate and multivariate analysis. All data were analyzed by SPSS statistical software and R software (http://www.r-project.org/).). After

Table 1
The primer sequences.

Gene name	Primer sequences (5'→3')
AKR1B10	F: CAGAAGACCCTTCCCTGCTG
	R: CGTTACAGGCCCTCCAGTTT
CD5L	F: CCTTCGGTCTTGCCTTTTGA
	R: GTGTCTCCTCCCACCAGCTT
LAPTM4B	F: GCGAGCTCTTCGCGGGGAGAG
	R: CAAGTACCAGACGCCGAGCAG
MMP9	F: CGCAGACATCGTCATCCAGT
	R: GGATTGGCCTTGGAAGATGA
SFN	F: GCCGAACGCTATGAGGACA
	R: GCTCAATACTGGACAGCACCC
SPP1	F: CGAGGTGATAGTGTGGTTTATGG
	R: GCACCATTCAACTCCTCGCTTTC
GAPDH	F: TGACAACTTTGGTATCGTGGAAGG
	R: AGGCAGGGATGATGTTCTGGAGAG

statistical treatment, $p < 0.05$, the difference was considered statistically significant.

3. Results

3.1. The Landscape of Immune Cells Infiltration and TME characteristics of HCC

In this study, a total of 131 HCC samples from TCGA and 167 HCC samples from GSE76427 were included. The abundance of tumor-infiltrating immune cells in HCC was determined using the CIBERSORT algorithm [33,34]. To describe the interindividual difference in the proportion of immune cell infiltration, unsupervised hierarchical clustering was performed on all samples. As shown in Fig. 1A, the heatmap displayed significant differences in 16 types of immune cell infiltration among these HCC samples with various clinicopathological characteristics. To describe the relationship between various immune cells in HCC, we constructed a correlation

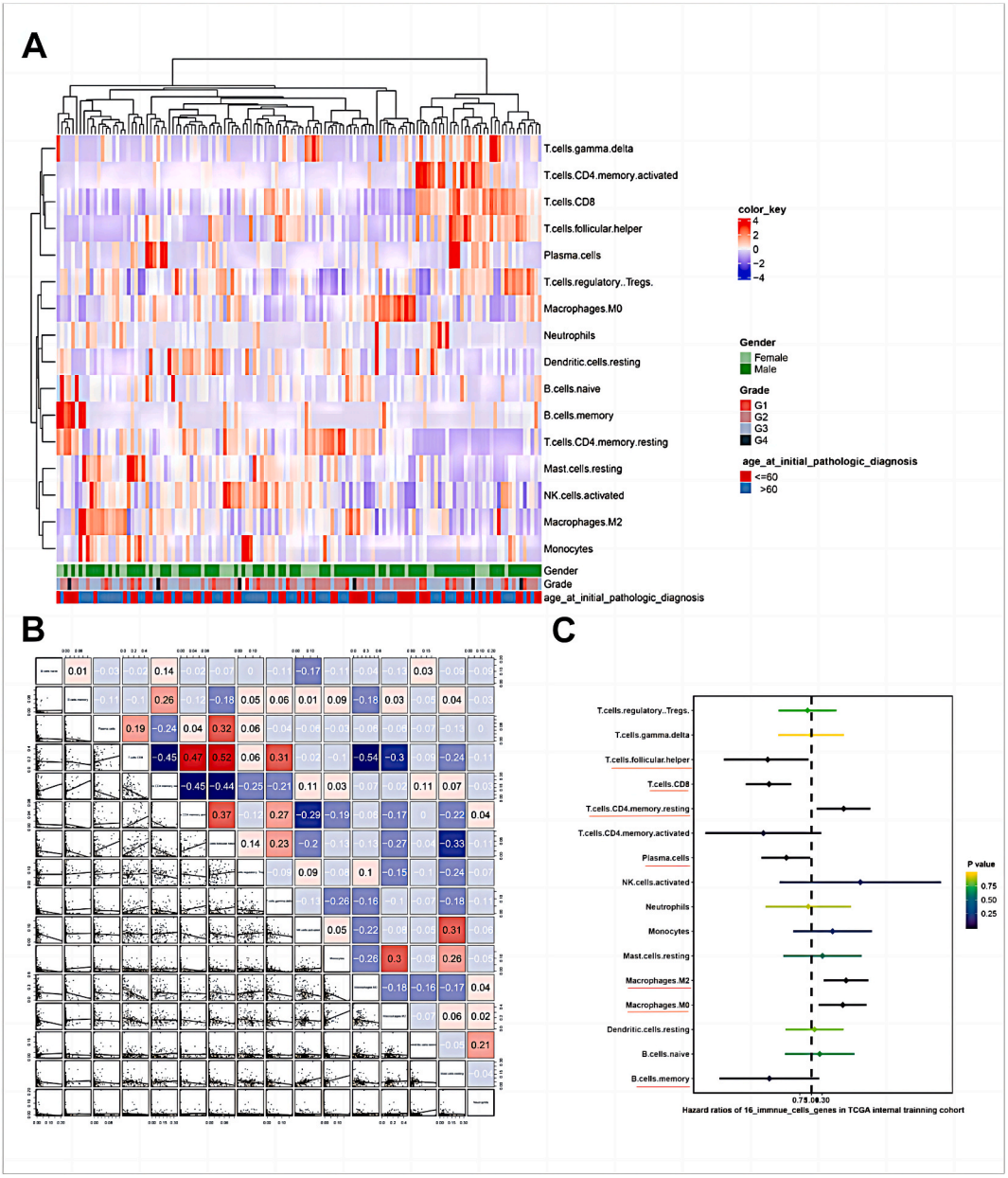

Fig. 1. The Landscape of Immune Cells Infiltration and TME characteristics of HCC. (A) Unsupervised clustering of 16 types of immune cell infiltration clusters among HCC patients from the TCGA cohort. (B) Correlation between 16 types of immune cells. (C) The forest plots of associations between different immune cells and Hazard ratios.

analysis between immune cells, as shown in Fig. 1B, $CD8^+$ T cells possessed a highly positive (r = 0.52) correlation with activated $CD4^+$ memory T cells and a highly negative (r = −0.54) correlation with M0 macrophages. To investigate the effects of various types of immune cells on clinical characteristics, we performed univariate Cox regression to identify whether immune cells can be an independent factor in predicting the prognosis of HCC patients. The forest plot showed that 7 of 16 types of immune cells are considered to be independent prognostic indicators for HCC patients (Fig. 1C).

3.2. Establishment and validation of immune-related prognostic model

To create a stable model to predict the risk for HCC patients, 131 HCC samples in the TCGA cohort were randomly divided into two groups: internal training cohort and validation cohort at 1:1. LASSO-Cox regression analysis, including 16 type immune cells, was

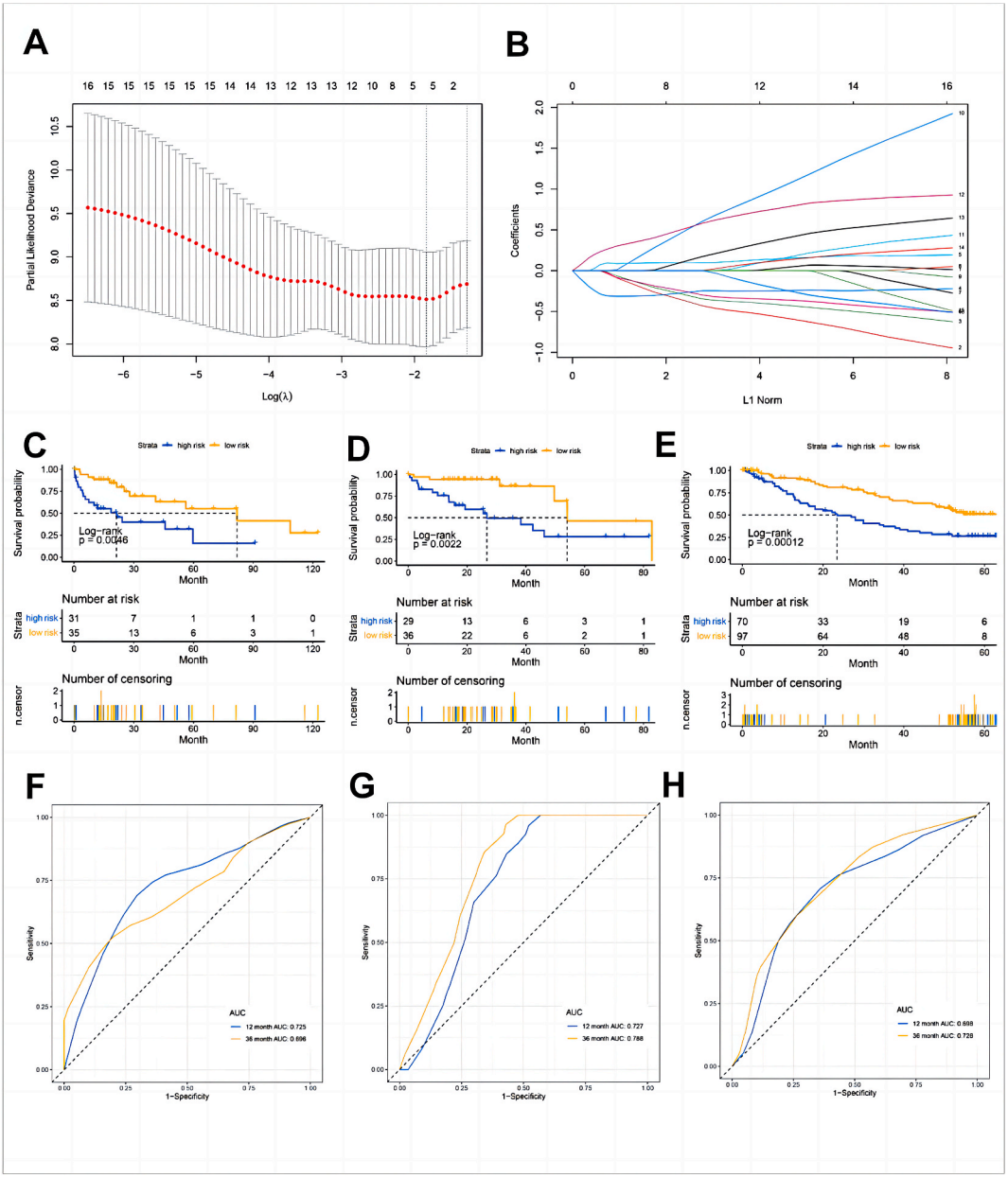

Fig. 2. Establishment and validation of immune-related prognostic model. (A, B) LASSO-Cox regression analysis identified 5 types of signature immune cells associated with HCC risk. (C–E) KM-curve for HCC patients with high and low risk in the internal training cohort, internal validation cohort, and external validation cohort respectively. (F–H) Receiver–operating characteristic (ROC) curves based on the prognostic immune risk score (pIRS) in the internal training cohort, internal validation cohort, and external validation cohort at 1 and 3 years respectively.

performed in the internal training cohort and identified 5 type signature immune cells associated with HCC risk (Fig. 2A and B), including 3 high-risk immune cells (T.cells.CD4.memory.resting, Macrophages.M0, Macrophages.M2) and 2 low-risk immune cells (Plasma. cells, T.cells.CD8). Therefore these 5 types of immune cells were used to establish the prognostic immune risk score (pIRS): pIRS = −0.2261 × fraction level of Plasma. cells + −0.450 × fraction level of T.cells.CD8 + 0.328 × fraction level of T.cells.CD4. memory. resting +0.555 × fraction level of Macrophages.M0 + 0.230 × fraction level of Macrophages.M2.

The Kaplan-Meier curves revealed that high pIRS indicated poor prognosis in TCGA training cohort (Fig. 2C). In addition, the pIRS also exhibited good performance in predicting prognosis in the internal validation cohort (Fig. 2D) and external validation cohort

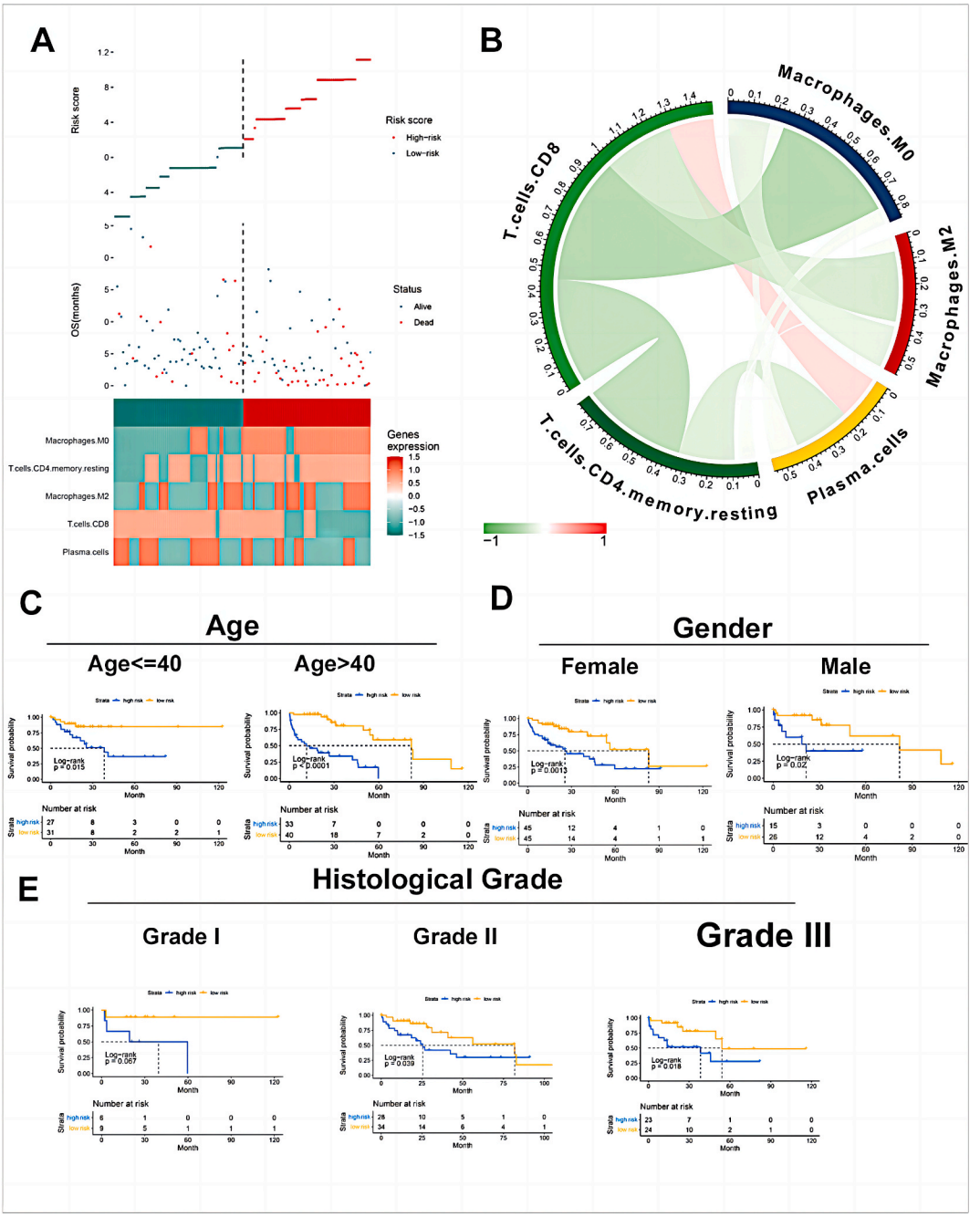

Fig. 3. The Correlation between the prognostic signature and clinicopathological characteristics. (A) Survival status and risk scores of HCC patients in the high- and low-risk groups in the internal training cohort. Green dots denote low risk and red dots denote high risk. (B) Correlation analysis of the 5 types of immune cells. (C–E) The Kaplan-Meier curve showed significant statistical differences in overall survival between high- and low-risk groups in different ages (C), sex (D), and histological grades (E).

(GSE14520, GSE76427, and GSE54236, Fig. 2E). The ROC curve at 1 and 3 years was generated and the AUC was 0.725 and 0.696 respectively (Fig. 2F), while they were 0.727, and 0.788 in the internal validation cohort (Figs. 2G), 0.698 and 0.726 in the external validation cohort respectively (Fig. 2H).

3.3. *The correlation between the prognostic signature and clinicopathological characteristics*

In addition, HCC patients in the internal training cohort were divided into low- and high-risk groups, based on the LASSO-Cox regression modeling by TCGA-HCC data in Fig. 2A and B. As shown in Fig. 3A, most of the high-risk groups have higher levels of T.cells.CD4.memory. resting, Macrophages.M2 and Macrophages.M2 infiltration, while lower levels of Plasma cells and T.cells.CD8 infiltration. Overall survival (OS) was longer in the low-risk group than in the high-risk group, which indicated that patients in the low-risk group had a better overall prognosis. Moreover, the correlation among the 5 immune cells in the signature was further discussed and there was a significantly positive correlation between T.cells.CD8 and Plasma cells (Fig. 3B).

Furthermore, we identified the reliability of the prognostic index in different subgroups according to patients' clinicopathological indicators. Survival analyses verified that the high-risk group had a worse survival outcome than the low-risk group, regardless of age, sex, or histological grade (Fig. 3C–E).

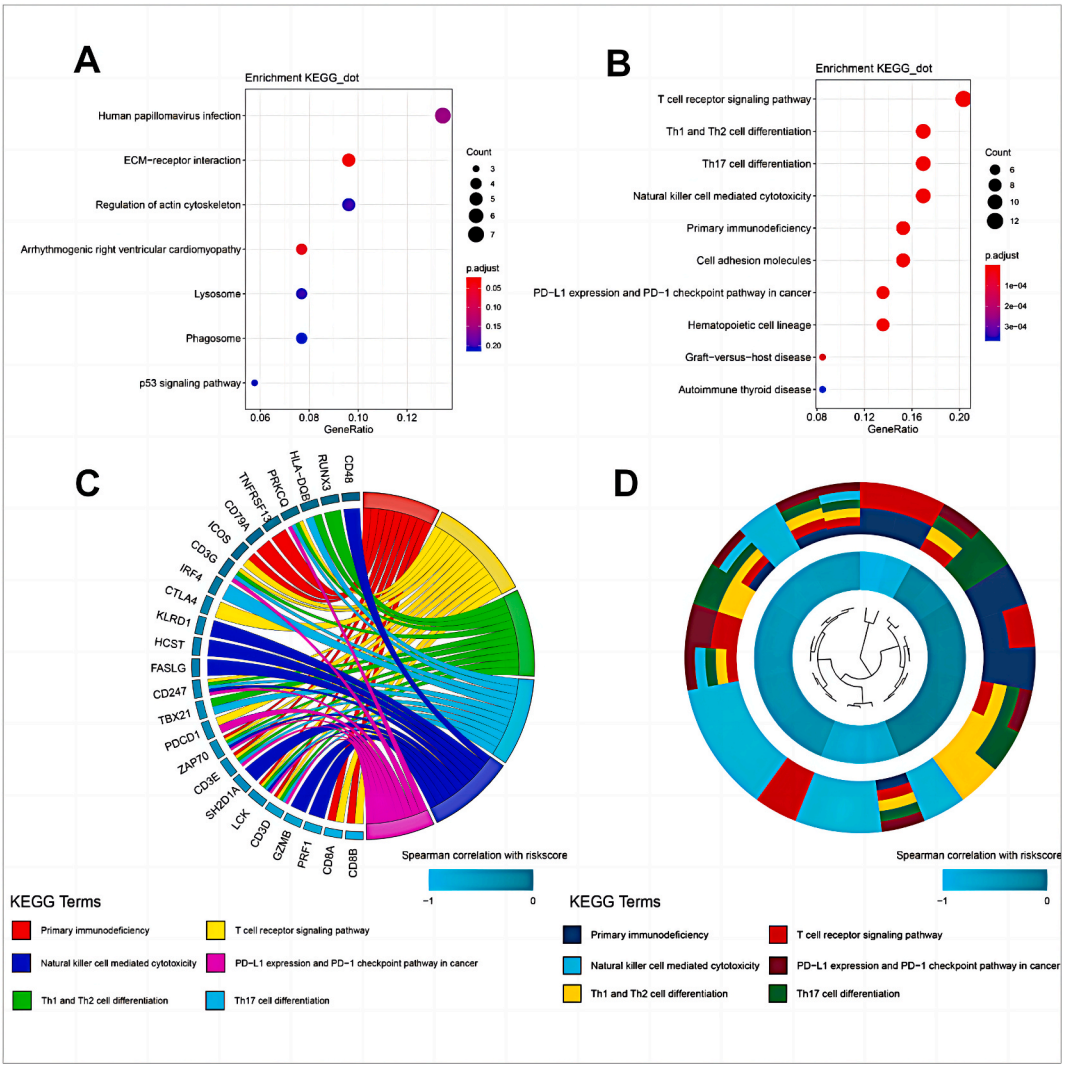

Fig. 4. Differentially Expressed Genes Analysis and Pathway Enrichment Analysis based on the prognostic signature. (A)KEGG analysis for the top 100 upregulated genes. (B) KEGG analysis for top 100 downregulated genes. (C, D) Chord plots show the association between genes and the KEGG pathways.

3.4. Differentially Expressed Genes Analysis and Pathway Enrichment Analysis based on the prognostic signature

To clarify the different biological characteristics of high- and low-risk patients, according to the characteristics of 5 types of immune cell signatures, Gene set enrichment analysis (GSEA) was carried out between genes and risk scores in TCGA cohort and genes with the top 100 positive and negative correlation were used to conducted KEGG enrichment analysis using clusterProfiler software package in R software. The differentially expressed genes between high and low groups showed that positive correlations genes were significantly enriched in ECM-receptor interaction, while negative correlations genes were significantly enriched in Th1 and Th2 cell differentiation and Primary immunodeficiency (Fig. 4A–D).

3.5. Identification of prognosis-associated genes in HCC

To identify genes significantly related to the prognosis of HCC, we conducted further analysis on TCGA and GSE14520 respectively. According to the risk score, HCC patients were divided into two groups with high- and low-risk, and the differentially expressed genes (DEGs) were screened. Comparing HCC samples with high-vs. low-risk (p.adjust <0.05 and $|\log2 \text{ fold change}| > 0.585$), we identified 232 DEGs in the TCGA cohort and 162 DEGs in the GSE14520 cohort (Fig. 5A–B). In addition, the Venn diagram showed 11 upregulated DEGs and 8 downregulated DEGs appearing in both TCGA and GSE14520 cohorts (Fig. 5C–D).

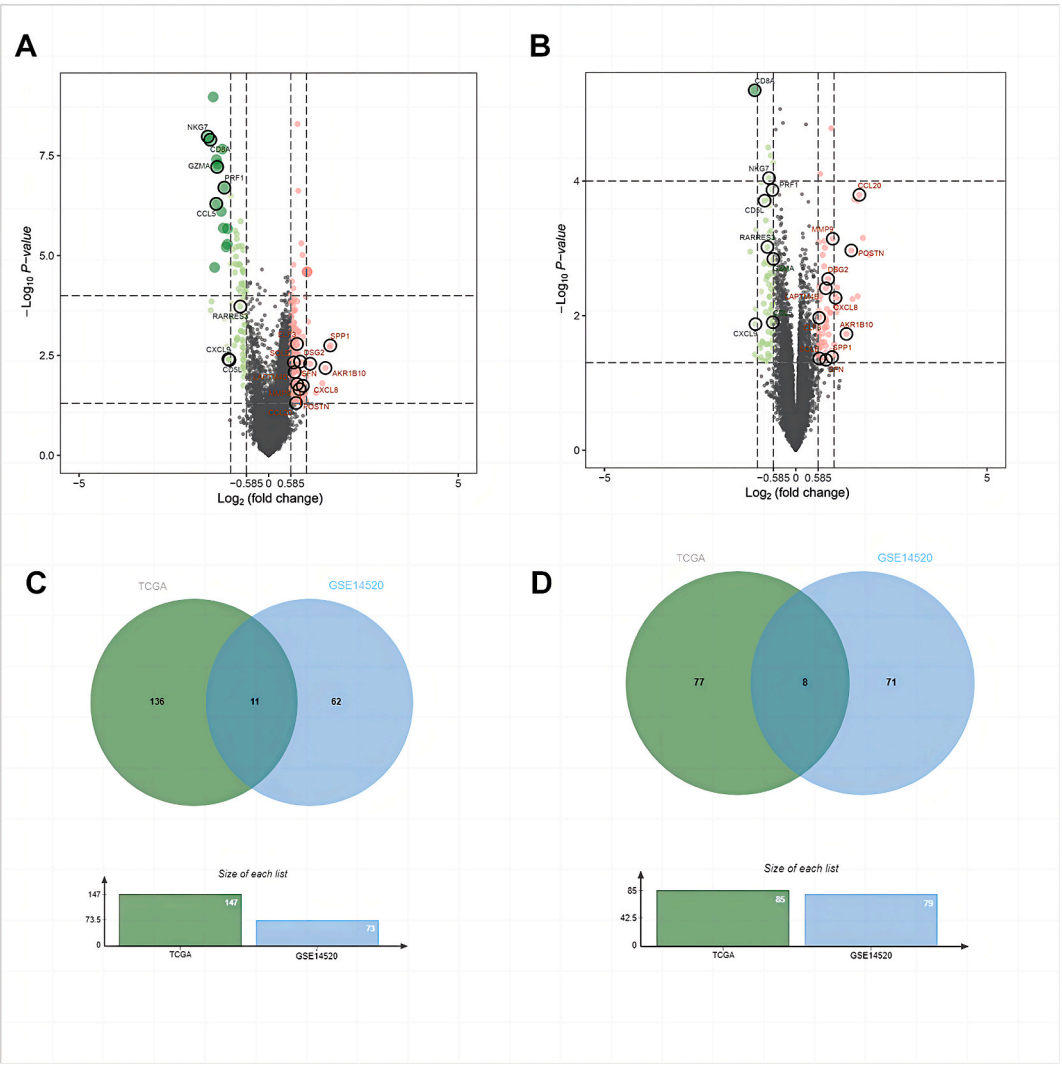

Fig. 5. Identification of prognosis-associated genes in HCC. According to the risk cores, HCC patients in TCGA and GSE14520 were divided into high- and low-risk groups, and the differentially expressed genes (DEGs) were performed. (A)The volcano Plot of differentially expressed genes between high- and low-risk groups in TCGA cohort (B) The volcano Plot of differentially expressed genes between high- and low-risk groups in GSE14520 cohort. The red circles represent up-regulated genes, and the green circles represent down-regulated genes. The Venn diagram shows the consistently up-regulated genes (C) and the consistently down-regulated genes (D) in the TCGA cohort and GSE14520 cohort.

To evaluate the prognostic value of these 19 DEGs in HCC, we further calculated the correlations of these 19 DEGs with overall survival (OS) of HCC patients from GEPIA databases, using the univariate Cox survival analysis. 11 DEGs were considered valuable that high expression of AKR1B10, CXCL8, ELF3, LAPTM4B, MMP9, NKG7, POSTN, SFN and SPP1 was strongly associated with poor patient outcomes in HCC, while low expression of CD5L and GZMA was strongly associated with good patient outcomes (Fig. 6 and Supplement Fig. 1).

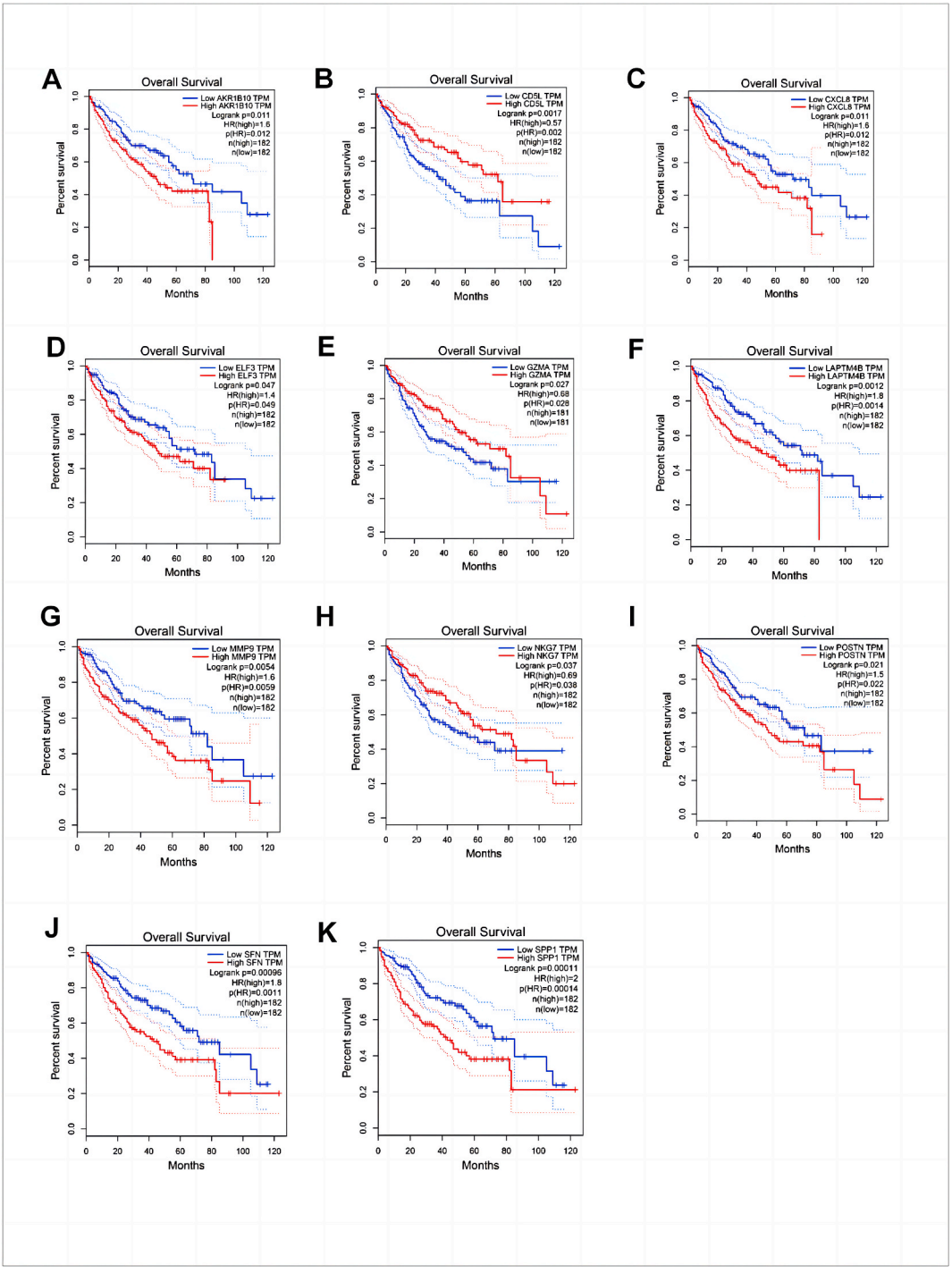

Fig. 6. Identification of prognosis-associated genes in HCC. According to the expression level of these differentially expressed genes (DEGs), the HCC patients were divided into high- and low-expression groups. Red represents high expression and blue represents low expression (A–K) Survival plots of high- and low-expression groups in the TCGA cohort.

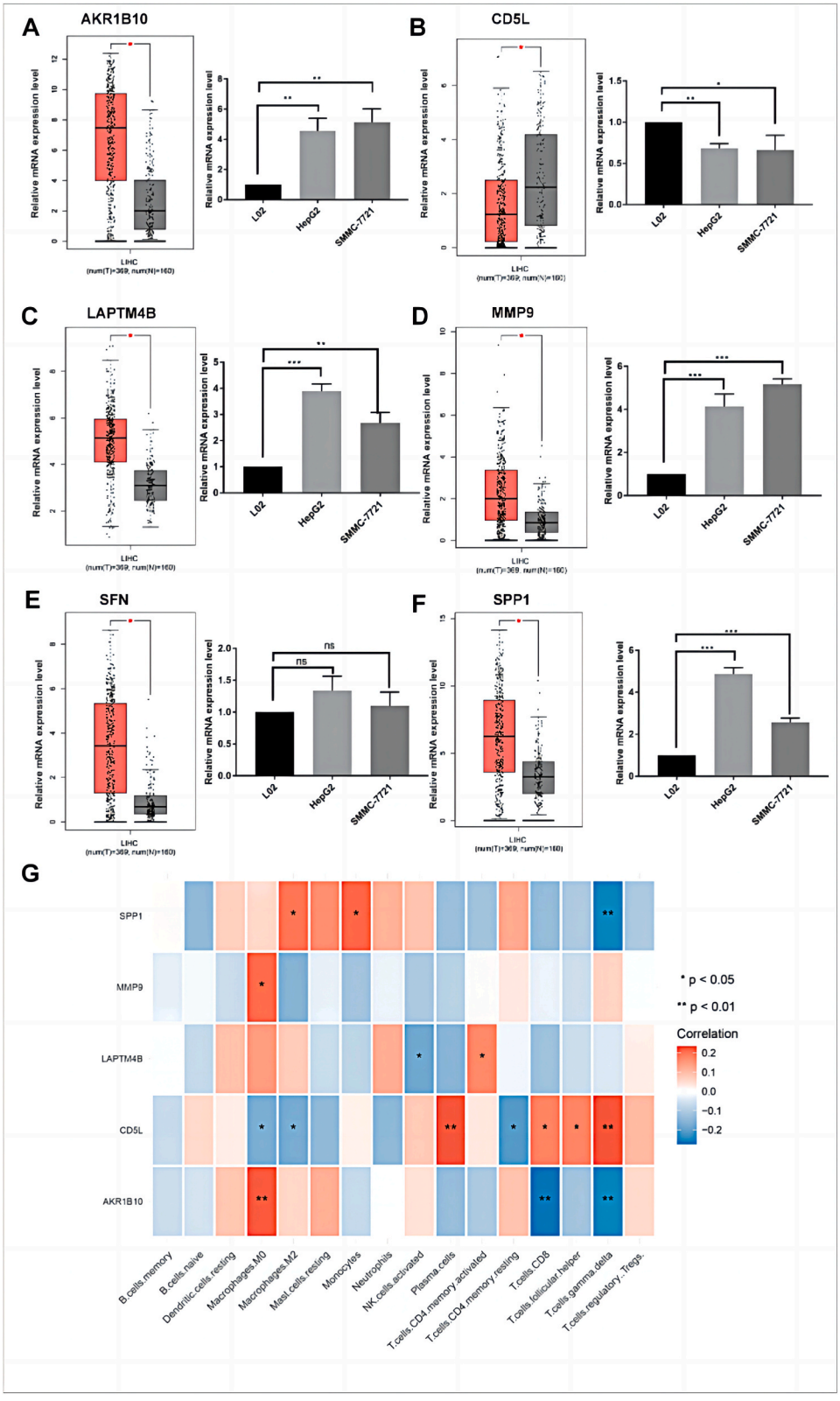

Fig. 7. Validation of gene expression in HCC. The box diagram on the left shows the difference in gene expression between normal tissues and HCC. The right side represents the difference in gene expression between normal liver cell lines and HCC cell lines. (A) For AKR1B10, (B) for CD5L, (C) for LAPTM4B, (D) for MMP9, (E) for SFN, (F) for SPP1 respectively. (G) The correlation between immune cells and 5 prognostic genes in HCC.

3.6. Validation of gene expression in HCC

To ensure positive confirmation of the pathophysiological roles of 11 DEGs, we applied experimental validation to investigate their clinicopathological characteristics. Bioinformatics analysis showed that the expression levels of AKR1B10, CD5L, LAPTM4B, MMP9, SFN, and SPP1 were significantly different between HCC and normal tissues (Fig. 7A–F and Supplement Fig. 2). Then, we performed qRT-PCR analyses in the normal liver cell line L02 and the liver cancer cell line HepG2, SMMC-7721 across AKR1B10, CD5L, LAPTM4B, MMP9, SFN and SPP1 (Fig. 7A–F). Results showed that the expression of AKR1B10, LAPTM4B, MMP9, and SPP1 in the HCC cell line was significantly higher than that in normal cells, while the expression of CD5L in the HCC cell line was significantly lower (Fig. 7A–F). We further analyzed the association between these 5 genes and immune cells and found that MMP9 and AKR1B10 are associated with high levels of M0 macrophage infiltration, while CD5L is associated with high levels of T. cells.CD8 and Plasma cell infiltration (Fig. 7G). These data suggested that AKR1B10, LAPTM4B, MMP9, CD5L, and SPP1 may serve as potential prognostic biomarkers in HCC.

4. Discussion

Hepatocellular carcinoma (HCC), the main type of liver cancer, is a challenging malignancy that poses a significant threat to human life due to the complexity of the molecular mechanisms underlying its progress. Previous studies have proved that HCC was mainly related to long-term inflammation, accompanied by infiltration of various types of immune cells into liver tissue. However, biomarkers that can be directly used to predict the prognosis of HCC patients remain to be explored. Compared with a single biomarker, the prognostic gene model may have a better predictive effect. With the deepening of research, gene markers based on mRNA are widely used in tumor prognosis prediction [35]. Moreover, during the occurrence and progression of tumors, the role of immune cells in the tumor microenvironment has been increasingly recognized [32,36-38]. However, a single immune cell is limited to predicting the prognosis of HCC patients and revealing the complete compositions in the HCC immune microenvironment.

Benefited the discovery of $CD4^+$ T cell subset-defining key transcription factors and framing of the Th1/Th2 paradigm, ample evidence has supported that tumor-infiltrating lymphocytes (TILs) are critical in regulating immune responses under pathological conditions, and play a prominent role in immune evasion, drug resistance, and promotion of cancer metastases [39–42]. Previous studies have identified 11 TILs of HCC, including many exhausted T cells. Researchers also found a massive immune cell ($CD4^+$ T cell, $CD8^+$ T cell, B cell, and macrophage) infiltration characterized the immune inflamed phenotype in HCC [30–32,43,44]. It is worth noting that the balance between immune cells is critical for immune homeostasis, such as a shift of Th1/Th2 balance towards Th2 cells is correlated with the immunosuppression and progression of cancer [45]. Yet, more exact mechanisms underpinning the effects of T cells on tumor immunity in HCC remain to be elucidated.

In our study, we used the CIBERSORT algorithm to explore the tumor-infiltrating immune cells and construct a stable prognostic value in HCC patients, based on public HCC RNA-seq data. Results of univariate analysis suggested 7 types of immune cells with significant prognostic value. Moreover, the lasso-cox model constructed a prognostic model of HCC based on these immune cells' landscape. Finally, a 5 immune cells signature (T.cells.CD4.memory. resting, Macrophages.M0, Macrophages.M2, Plasma. cells, and T. cells.CD8) was constructed (Fig. 2). This signature showed good performance in the prediction of 1-year and 3-year survival rates in the internal training cohort, internal validation cohort, and external validation cohort. Further subgroup analysis found that the model has general applicability among people of different genders, ages, and pathological stages (Fig. 3), which suggests that our model has a stable value for predicting the prognosis of HCC.

In addition, further differential gene analysis and PCR analysis revealed that 5 genes including AKR1B10, LAPTM4B, MMP9, SPP1, and CD5L are unusually expressed in HCC, which will help follow-up in-depth research on the HCC mechanism. Newly studies have reported that AKR1B10 and SPP1 may possess possible interactive networks with immune cells [43]. Our research further reveals that AKR1B10 may be involved in regulating the biological behavior of M0 macrophages in HCC. We also found that LAPTM4B may inhibit the activation of NK cells in HCC, which has not been reported. Yet, more exact mechanisms underpinning the effects of these 5 genes, including AKR1B10, LAPTM4B, MMP9, SPP1, and CD5L, on tumor immunity remain to be elucidated.

Compared with previous studies, we constructed a novel prognostic index, based on 5 types of immune cells, to predict the prognosis and immunotherapy efficacy of HCC patients, and it was well-validated from multiple aspects. Nonetheless, several limitations were notable in our study. Due to all data being collected retrospectively from public databases, the potential bias of clinicopathological features is inevitable. Thus, large, random, multicenter prospective clinical trials are needed to support our findings, the reliability of our prognostic index, and the expression levels of 5 prognosis-associated genes in HCC. We selected only patients with RNA-seq data to analyze prognostic immune risk scores in HCC, this selection bias might cause prediction errors for signatures. So, we need more studies to verify and improve the predictive power of the diagnostic score.

Cancer immunotherapies, especially immune checkpoint blockade therapy, have transformed cancer treatment by promoting complete and durable responses and are now the standard treatment for various malignancies. Unfortunately, due to limited immune activation to recognize tumor-specific antigens, only a small population of patients with certain cancer types respond to immunotherapy efficiently. Therefore, it is essential to identify additional potential therapeutic targets. Our current research showed that immune cell infiltration-related genes demonstrated strong correlations with HCC patient outcomes. In consequence, the present study points new directions for delineating the relationships between the immune cell infiltration-related genes within the TME, which may have important implications for exploring new strategies for cancer therapy.

5. Conclusions

Our results systematically demonstrated the infiltration of 5 types of immune cells in HCC and established a stable predictive prognostic immune signature in HCC. AKR1B10, LAPTM4B, MMP9, SPP1, and CD5L are expected to become markers and therapeutic targets for predicting the prognosis of HCC.

Funding

This work was supported by grants from Education and Teaching Research Project of Chifeng University (JYXMZ202101, JYXMZ202103), Applied Demonstration courses of Chifeng University (SFK20211401), Course network teaching resource construction project of Chifeng University (WL202021), Young Scholar Program of Chifeng University (CFXYQN202141), The Inner Mongolia Social Science Foundation (2022DY22) and Inner Mongolia Department of Education (NJZY22143, NJZY22182, NJZY23038).

Data availability

All data generated or analyzed during this study are included in this published article. The datasets presented in this study can be found in online repositories. The names of the repository/repositories and accession number(s) can be found in the article/Supplementary Material.

Ethics approval and consent to participate

Not applicable.

Patient consent for publication

Not applicable.

CRediT authorship contribution statement

Hongru Cao: Software, Data curation, Conceptualization. **Ping Huang:** Software, Project administration, Formal analysis, Conceptualization. **Jiawei Qiu:** Formal analysis, Data curation. **Xiaohui Gong:** Writing – review & editing, Writing – original draft, Supervision, Funding acquisition, Conceptualization. **Hongfei Cao:** Writing – review & editing, Funding acquisition, Data curation.

Declaration of competing interest

The authors declare that they have no known competing financial interests or personal relationships that could have appeared to influence the work reported in this paper.

Acknowledgments

All authors acknowledge the contributions from the TCGA, GEO, and ICGC project.

Appendix A. Supplementary data

Supplementary data to this article can be found online at https://doi.org/10.1016/j.heliyon.2024.e24861.

References

[1] A. Forner, M. Reig, J. Bruix, Hepatocellular carcinoma, Lancet 391 (10127) (2018) 1301–1314.
[2] H. Sung, et al., Global cancer Statistics 2020: GLOBOCAN estimates of incidence and mortality worldwide for 36 cancers in 185 countries, CA Cancer J Clin 71 (3) (2021) 209–249.
[3] F. Ebrahimi, et al., Familial coaggregation of MASLD with hepatocellular carcinoma and adverse liver outcomes: nationwide multigenerational cohort study, J. Hepatol. (2023).
[4] H. Rumgay, et al., Global burden of primary liver cancer in 2020 and predictions to 2040, J. Hepatol. 77 (6) (2022) 1598–1606.
[5] European Association for the Study of the Liver, Electronic address, e.e.e. and L. European Association for the Study of the, EASL Clinical Practice Guidelines: Management of hepatocellular carcinoma. J Hepatol 69 (1) (2018) 182–236.
[6] J. Zheng, et al., Actual 10-year survivors after resection of hepatocellular carcinoma, Ann. Surg Oncol. 24 (5) (2017) 1358–1366.
[7] J.M. Llovet, A. Burroughs, J. Bruix, Hepatocellular carcinoma, Lancet 362 (9399) (2003) 1907–1917.
[8] J. Bruix, M. Sherman, A.A. f.t, S.o.L.D. Practice, Guidelines committee, Management of hepatocellular carcinoma. Hepatology 42 (5) (2005) 1208–1236.
[9] J. Bruix, et al., Clinical management of hepatocellular carcinoma. Conclusions of the barcelona-2000 EASL conference. European association for the study of the liver, J. Hepatol. 35 (3) (2001) 421–430.
[10] G. Spinzi, S. Paggi, Sorafenib in advanced hepatocellular carcinoma, N. Engl. J. Med. 359 (23) (2008) 2497–2498, author reply 2498-9.

[11] G.K. Abou-Alfa, et al., Doxorubicin plus sorafenib vs doxorubicin alone in patients with advanced hepatocellular carcinoma: a randomized trial, JAMA 304 (19) (2010) 2154–2160.
[12] F. Finkelmeier, et al., Feasibility and safety of nivolumab in advanced hepatocellular carcinoma: real-life experience from three German centers, J. Cancer Res. Clin. Oncol. 145 (1) (2019) 253–259.
[13] S. Kambhampati, et al., Nivolumab in patients with advanced hepatocellular carcinoma and Child-Pugh class B cirrhosis: safety and clinical outcomes in a retrospective case series, Cancer 125 (18) (2019) 3234–3241.
[14] A.B. El-Khoueiry, et al., Nivolumab in patients with advanced hepatocellular carcinoma (CheckMate 040): an open-label, non-comparative, phase 1/2 dose escalation and expansion trial, Lancet 389 (10088) (2017) 2492–2502.
[15] T. Yau, et al., Efficacy and safety of nivolumab plus ipilimumab in patients with advanced hepatocellular carcinoma previously treated with sorafenib: the CheckMate 040 randomized clinical trial, JAMA Oncol. 6 (11) (2020) e204564.
[16] H. Hackl, et al., Computational genomics tools for dissecting tumour-immune cell interactions, Nat. Rev. Genet. 17 (8) (2016) 441–458.
[17] R.S. Finn, et al., Atezolizumab plus bevacizumab in unresectable hepatocellular carcinoma, N. Engl. J. Med. 382 (20) (2020) 1894–1905.
[18] C. Engblom, C. Pfirschke, M.J. Pittet, The role of myeloid cells in cancer therapies, Nat. Rev. Cancer 16 (7) (2016) 447–462.
[19] J. Prieto, I. Melero, B. Sangro, Immunological landscape and immunotherapy of hepatocellular carcinoma, Nat. Rev. Gastroenterol. Hepatol. 12 (12) (2015) 681–700.
[20] H.U. Kasper, et al., Liver tumor infiltrating lymphocytes: comparison of hepatocellular and cholangiolar carcinoma, World J. Gastroenterol. 15 (40) (2009) 5053–5057.
[21] I.G. House, et al., Macrophage-derived CXCL9 and CXCL10 are required for antitumor immune responses following immune checkpoint blockade, Clin. Cancer Res. 26 (2) (2020) 487–504.
[22] W. Zhang, et al., IMonitor: a robust pipeline for tcr and BCR repertoire analysis, Genetics 201 (2) (2015) 459–472.
[23] T.L. Stephen, et al., Transforming growth factor beta-mediated suppression of antitumor T cells requires FoxP1 transcription factor expression, Immunity 41 (3) (2014) 427–439.
[24] I. Tirosh, et al., Dissecting the multicellular ecosystem of metastatic melanoma by single-cell RNA-seq, Science 352 (6282) (2016) 189–196.
[25] Y. Sun, et al., Single-cell landscape of the ecosystem in early-relapse hepatocellular carcinoma, Cell 184 (2) (2021) 404–421 e16.
[26] P. Savas, et al., Single-cell profiling of breast cancer T cells reveals a tissue-resident memory subset associated with improved prognosis, Nat Med 24 (7) (2018) 986–993.
[27] V. Chew, et al., Chemokine-driven lymphocyte infiltration: an early intratumoural event determining long-term survival in resectable hepatocellular carcinoma, Gut 61 (3) (2012) 427–438.
[28] W.Y. Cai, et al., Identification of a tumor microenvironment-relevant gene set-based prognostic signature and related therapy targets in gastric cancer, Theranostics 10 (19) (2020) 8633–8647.
[29] Q. Zhang, et al., Landscape and dynamics of single immune cells in hepatocellular carcinoma, Cell 179 (4) (2019) 829–845, e20.
[30] C. Zheng, et al., Landscape of infiltrating T cells in liver cancer revealed by single-cell sequencing, Cell 169 (7) (2017) 1342–1356, e16.
[31] X. Guo, et al., Global characterization of T cells in non-small-cell lung cancer by single-cell sequencing, Nat Med 24 (7) (2018) 978–985.
[32] X. Qu, et al., M2-like tumor-associated macrophage-related biomarkers to construct a novel prognostic signature, reveal the immune landscape, and screen drugs in hepatocellular carcinoma, Front. Immunol. 13 (2022) 994019.
[33] A.M. Newman, et al., Robust enumeration of cell subsets from tissue expression profiles, Nat. Methods 12 (5) (2015) 453–457.
[34] L. Li, et al., Evaluating distribution and prognostic value of new tumor-infiltrating lymphocytes in HCC based on a scRNA-seq study with CIBERSORTx, Front. Med. 7 (2020) 451.
[35] M. Jamal-Hanjani, et al., Translational implications of tumor heterogeneity, Clin. Cancer Res. 21 (6) (2015) 1258–1266.
[36] J. Bruix, G.J. Gores, V. Mazzaferro, Hepatocellular carcinoma: clinical frontiers and perspectives, Gut 63 (5) (2014) 844–855.
[37] P.H.D. Nguyen, et al., Intratumoural immune heterogeneity as a hallmark of tumour evolution and progression in hepatocellular carcinoma, Nat. Commun. 12 (1) (2021) 227.
[38] V. Thorsson, et al., The immune landscape of cancer, Immunity 48 (4) (2018) 812–830 e14.
[39] E.J. Wherry, M. Kurachi, Molecular and cellular insights into T cell exhaustion, Nat. Rev. Immunol. 15 (8) (2015) 486–499.
[40] K.E. Pauken, E.J. Wherry, SnapShot: T cell exhaustion, Cell 163 (4) (2015) 1038–1038 e1.
[41] S. Patil, R.S. Rao, B. Majumdar, T-Cell exhaustion and cancer immunotherapy, J. Int. Oral Health 7 (8) (2015) i–ii.
[42] D.W. Ho, et al., Single-cell RNA sequencing shows the immunosuppressive landscape and tumor heterogeneity of HBV-associated hepatocellular carcinoma, Nat. Commun. 12 (1) (2021) 3684.
[43] F. Zeng, et al., Predicting non-alcoholic fatty liver disease progression and immune deregulations by specific gene expression patterns, Front. Immunol. 11 (2020) 609900.
[44] L. Liu, et al., CD8+ T cell trajectory subtypes decode tumor heterogeneity and provide treatment recommendations for hepatocellular carcinoma, Front. Immunol. 13 (2022) 964190.
[45] J. Galon, D. Bruni, Tumor immunology and tumor evolution: intertwined histories, Immunity 52 (1) (2020) 55–81.